Int. J. Heat Mass Transfer. Vol. 10, pp. 181–194. Pergamon Press 1967. Printed in Great Britain

DIFFUSION FROM A GROUND LEVEL LINE SOURCE INTO THE DISTURBED BOUNDARY LAYER FAR DOWNSTREAM FROM A FENCE

ERICH J. PLATE
Fluid Dynamics and Diffusion Laboratory, Colorado State University

(*Received* 31 *January* 1966 *and in revised form* 3 *June* 1966)

Abstract—The concentration field is discussed which exists far downstream from a line source of ammonia gas emitting continuously into the boundary layer along a smooth flat plate. The boundary layer is obstructed by an impermeable and sharp-edged fence which extends over the whole width of the plate at a short distance downstream from the source. The basis of discussion is a set of experimental data which was obtained in a wind tunnel.

The flow field downstream from the fence exhibits three different zones of velocity distributions. These zones are indicated and a velocity distribution law is given based on the assumption that the disturbed boundary layer consists of two parts: an outer layer for which the parameters of the distribution law depend on the boundary-layer thickness and on the geometry of the disturbing fence, and an inner layer for which the velocity distribution law depends on the roughness of the floor.

The vertical distributions of concentrations downstream from the fence follow a similarity law whose shape corresponds to that found in undisturbed boundary layers. The similarity parameters reflect strongly the presence of the fence. The characteristic length λ is found to increase exponentially with the fence height. The characteristic length, the similarity law, and the velocity distribution law, are used to calculate the maximum ground concentrations at large distances downstream from the fence where the presence of the boundary-layer edge limits the growth of the diffusion plume to that of the boundary layer.

NOMENCLATURE

- A, coefficient in the velocity distribution law for the outer layer [Dimensionless];
- c, local concentration [cm^3/cm^3];
- c_f, shear-stress coefficient of the outer layer [Dimensionless];
- c_{max}, maximum or ground-level concentration [cm^3/cm^3];
- D, coefficient in the velocity distribution law for the inner layer [Dimensionless];
- G, volume flow rate of diffusing gas per unit width of line source [$cm^3/s\,cm$];
- h, fence height [cm];
- I_1, I_2, integrals in the determination of ground level concentrations [Dimensionless];
- k, Von Kármán's constant [Dimensionless];
- L, distance of reattachment point from fence [cm];
- u, local velocity [cm/s];
- u_{*i}, shear velocity of inner layer [cm/s];
- u_{*o}, shear velocity of outer layer [cm/s];
- u_a, ambient velocity [cm/s];
- x, horizontal distance from the source [cm];
- x', ratio δ'/δ [Dimensionless];
- X, horizontal distance from the fence [cm];
- y, vertical distance from the wall [cm];
- z_o, roughness height [cm].

Greek symbols

- α, exponent in concentration distribution law [Dimensionless];
- λ, distance y at which $c = \frac{1}{2} c_{max}$ [cm];
- ν, kinematic viscosity [cm^2/s];
- δ, boundary-layer thickness [cm];

δ_o, thickness of the undisturbed boundary layer at $X = 0$ [cm];
δ', thickness of inner boundary layer [cm];
ρ, density of air [g/cm^3];
τ_o, wall shearing stress [g/cm^2].

INTRODUCTION

THE ATMOSPHERIC boundary layer hardly ever corresponds to the aerodynamic flow along a flat plate with uniform roughness. Changes of roughness along the approach distance, and topographic features of small or large dimensions, cannot fail to show their influence in the local flow characteristics, and therefore, also in the distribution of concentrations of any matter which happens to be present in the atmosphere. Very little is known about the flow in a boundary layer which is disturbed by a topographic feature and even less about diffusion in such a flow field.

In order to provide a body of experimental data, against which hypotheses concerning diffusion of gas in a disturbed boundary layer can be tested, the experiments reported herein were undertaken. As a first experimental set-up, the obstacle chosen consisted of a sharp-edged flat plate placed perpendicular to the direction of flow, and extending over the whole width of the test section of a low speed wind tunnel. This type of obstacle shall be called a fence. The physical situation corresponds somewhat to the atmospheric flow over wind breaks or snow fences, but other types of obstacles can be expected to behave similarly.

The diffusion plume was emitted continuously from a line source placed at some distance upstream from the fence at ground level, as is indicated in Fig. 1. The floor of the wind tunnel test section represents the lower boundary of the flow field on which the boundary layer is forming. The basic variable for the present study of the diffusion field was the height of the fence.

THE DIFFUSION ZONES OF A DISTURBED BOUNDARY LAYER

An analytical description of the mean concentration distribution of a contaminating gas, downstream from a continuous source, requires a determination of the probability distribution for finding contaminants at a given point in space downstream from the source. This probability distribution is related to the velocity field because it denotes the relative number of elementary parcels of contaminating gas which have travelled from the vicinity of the source to the space point considered. Clearly, the path of travel is the time integral of the instantaneous velocities of the parcels with contaminating gas. If the gas only marks, rather than modifies the velocity field of the carrier fluid, then the velocities of the parcel are the Lagrangian velocities of the turbulence field of the carrier fluid. This view of turbulent diffusion, due to Taylor [1], indicates immediately the difficulties inherent in each analytical description of a

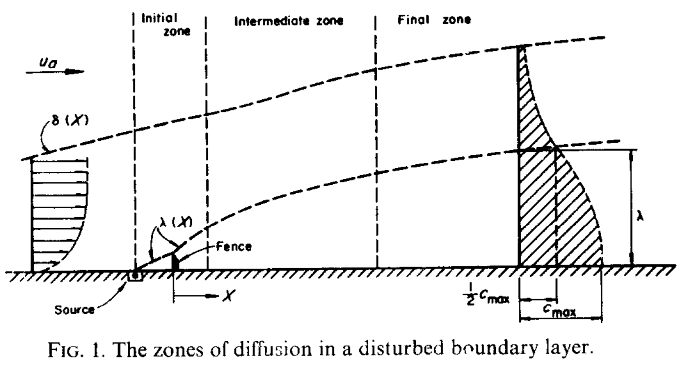

FIG. 1. The zones of diffusion in a disturbed boundary layer.

turbulent diffusion process, because even the determination of the mean concentration requires the averaging of a large number of realizations of the Lagrangian turbulence field. A solution of the equations which relate the statistical parameter of the flow turbulence to the mean concentration distribution has, therefore, been obtained only for simple cases of homogeneous turbulence. Semi-empirical equations, based on experimental evidence, are required for more complicated flow situations.

In an undisturbed boundary layer, it is found that both the distribution of velocity and of mean concentrations follow a similarity law. The logarithmic velocity distribution law for a rough boundary:

$$\frac{u}{u_{*i}} = \frac{1}{k}\ln\frac{y}{z_o} \tag{1}$$

holds in the constant stress layer near the boundary. In this equation u_{*i} is the shear velocity based on the wall shearing stress $\tau_o = \rho u_{*i}^2$, and z_o is the roughness height which indicates the roughness characteristics of the boundary. This law is, however, not valid everywhere in the boundary layer. In the outer layer of the constant stress region, the velocity defect law

$$\frac{u - u_a}{u_{*i}} = \frac{1}{k}\ln\frac{y}{\delta} \tag{2}$$

describes the distribution of velocity, where u_a is the velocity outside of the boundary layer, and δ is the boundary-layer thickness. As was shown by Clauser, equation (2) reflects the momentum defect due to the shearing stress ρu_{*i}^2 of the portion of the wall which lies at a large distance upstream from the section considered [2]. The logarithmic law is the equilibrium form of the velocity distribution in a turbulent boundary layer, and any constant stress boundary layer adjusts to it. Therefore, one can expect to find that at large distances downstream from a fence the outer profile has a shape like that of equation (2), but with u_{*i} replaced by another shear velocity u_{*o} which represents the effect of the fence. In addition, for a disturbed boundary layer, the boundary-layer thickness δ is different from that of an undisturbed boundary layer.

In an undisturbed boundary layer, the mean concentrations follow a similarity distribution. For the mean concentrations downstream from a line source at ground level, Wieghardt [3], and Poreh and Cermak [4], among others, show evidence that the distribution of temperature and of mass concentration, emitted respectively from a line source of heat and of ammonia, are represented by a similarity distribution of the form

$$\frac{c(x, y)}{c_{\max}(x)} = e^{-\ln 2\left(\frac{y}{\lambda(x)}\right)^{\alpha}} \tag{3}$$

where the exponent α was found to be about 1·6 to 1·8. In this equation, $c(x, y)$ stands for concentration (or temperature excess), $c_{\max}(x)$ is the concentration (or temperature excess) at ground level at some distance x, and $\lambda(x)$ is defined as that vertical distance at which the concentration in the two-dimensional concentration plume is reduced to one-half its value at the boundary for given x, as indicated in Fig. 1.

The diffusion characteristics depend on the distance x of the section at which measurements are being taken from the source. This has been demonstrated by Poreh and Cermak [4]. They separated the diffusion field into the zones indicated in Fig. 1. In the first zone, near the source, the geometry of the source and the local velocity gradients are of dominant influence. In the second zone, the diffusion cloud spreads out according to the law:

$$\lambda(x) = 0{\cdot}076\, x^{0{\cdot}8} \tag{4}$$

where both λ and the distance x from the source are given in cm. The exponent of 0·8 is apparently characteristic for all types of boundary-layer disturbances in an equilibrium layer. It is well known that the same exponent is found when the growth of a turbulent boundary layer along a smooth surface is determined from Blasius' velocity distribution law (see reference [5]). An exponent of 0·8 was also found by Elliott for his model of the growth of an internal boundary layer which starts at the discontinuity in roughness between two adjacent surfaces of uniform but unequal roughness [6]. Boundary layers and diffusion clouds of two-dimensional mean flows, are thus found to obey the same growth laws. Explanations of this feature have been given for the diffusion characteristics in terms of the Lagrangian similarity hypothesis [7] and in terms of a two-layer model of turbulent flows over walls with roughness discontinuities for the velocity distributions [8, 9].

Similar developments are found when the boundary layer is disturbed by a fence. However, one must expect that in the intermediate zone λ grows slower than in the case of an undisturbed boundary layer, because the high turbulence level which was generated by the separation from the fence edge decays quite rapidly. For the present experiments, it is not possible to determine the growth rate of λ in the intermediate zone with any certainty; it appears that the final zone develops directly after the initial zone.

In the final region of an undisturbed boundary layer the diffusion parameter λ becomes proportional to the boundary-layer thickness δ, with a factor of proportionality between λ and δ of about 0·64. According to Poreh and Cermak, at a large distance from the source, the growth of the diffusion cloud is limited because outside of the boundary layer the turbulence level is very low and all diffusion takes place essentially by molecular action [4]. Consequently, only very little gas (or heat) is lost to the flow outside of the boundary layer.

The same result is found for a boundary layer which is disturbed by a fence, as will be shown. This permits to obtain a complete set of equations for the final zone diffusion from reasonable, but empirical equations for the boundary-layer velocity distributions, the growth of the boundary layer, and the concentration–distribution law. From these, the ground level concentrations can be determined for the final zone and compared with experimental results, as will be done in the remainder of the paper.

EXPERIMENTAL PROCEDURES

The experiments were performed in a non-circulating low-speed wind tunnel, which was formerly located in the Fluid Mechanics and Diffusion Laboratory of Colorado State University. An air velocity of about 2·7 m/s was used for the diffusion experiments. Fence heights of 1·27, 2·54, 3·81 and 5·08 cm were studied. The line source of gas was located at a distance of 9 m downstream from the test section entrance and 0·46 m upstream from the fence. The fence consisted of angle iron pieces with machined sharp edges.

No reliable measurements of the velocity distributions were taken during the time of the concentration measurement. The measurements suffice, however, to show the development of the outer edge of the boundary layer. After these measurements, the wind tunnel was torn down. The velocity field downstream from a fence was, later on, investigated by Plate, in a new wind tunnel, over a wide range of variables, and the discussion of the velocity distributions is based on the later results [10]. The velocity distributions were measured with a pitot static tube in conjunction with an electronic micromanometer (Transonics Equibar Type 120) which was calibrated periodically against a water manometer (Flow Corporation Type MM2).

The gas consisted of anhydrous ammonia, which was emitted continuously from a 4-ft long-line source at ground level. The source produced a mean concentration field which was nearly two-dimensional, except near the wind tunnel walls.

Concentrations were measured by passing air–gas mixtures, withdrawn continuously from the wind tunnel at the desired point by means of a vacuum pump, through a known volume of hydrochloric acid, which absorbed the ammonia over a fixed period of time, usually 1 min.

An addition of Nessler's Reagent to the sample gave a brown discoloration which, in a colorimeter, yielded a light absorption proportional to the concentration of ammonia trapped in the sample over a given period of time. The procedure is accurate within ± 20 per cent at readings of 500 ppm. An uncertainty of the data of about ± 30 ppm has to be expected for all readings. Measurements of low concentrations are, therefore, very unreliable. The sampling system has been described by Malhotra and Cermak [11]. Poreh and Cermak gave the details of the source and of the wind tunnel [4].

VELOCITY DISTRIBUTIONS IN THE DISTURBED BOUNDARY LAYER

The velocity field downstream from the fence is distorted by the presence of the fence. One can distinguish the different flow zones indicated in Fig. 2. These flow zones are separated by suitable blending regions.

At some distance upstream from the fence, the boundary layer is unaffected by the presence of the fence and behaves like an undisturbed boundary layer along a smooth flat plate. At a short distance in front of the fence, the boundary layer separates and a separation bubble with a closed circulation is formed. The separation streamline reattaches on the front of the fence, at a point close to the fence edge. At the fence edge the flow separates again, this time forming a much longer separation zone. Reattachment takes place at $X = L$ and along the plate for $X > L$ a new inner boundary layer is developing which gradually thickens. The outer portion of the boundary layer in this region remains essentially unchanged, except for an outward displacement. With further increase in distance, the blending region between the inner and outer layer increases in width, and there is some experimental evidence that at some large value of X the blending profile has spread over the whole boundary layer, and determines the velocity distribution in the redeveloped boundary layer. Ultimately, only the increased boundary-layer thickness remains as an indication of the distortions which the flow field suffered by the fence.

The flow region near separation is governed by both the velocity field and the pressure field which is created by the retardation and acceleration of the fluid near the fence. Downstream from reattachment, the pressure again becomes constant, and, from then on, one may expect that the boundary layer develops in the form of an outer displaced equilibrium layer and an inner equilibrium boundary layer [8]. Since equilibrium layers in wall shear flows obey to a good approximation, logarithmic velocity distribution laws, the velocity distributions are best presented in a semi-logarithmic plot. Examples are shown in Fig. 3. In this figure, dimensionless velocities obtained by dividing the local velocity u by the ambient velocity u_a were plotted against

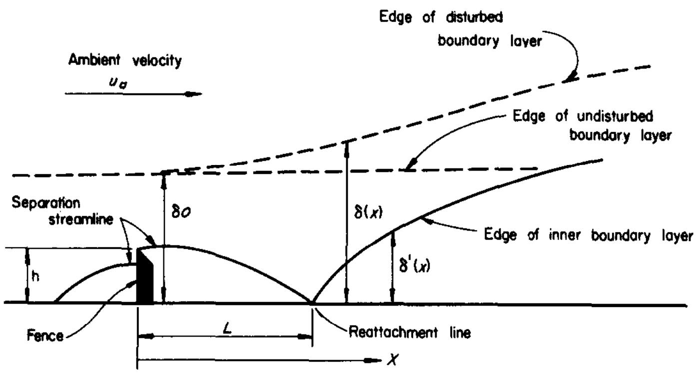

FIG. 2. Flow regions of the disturbed boundary layer.

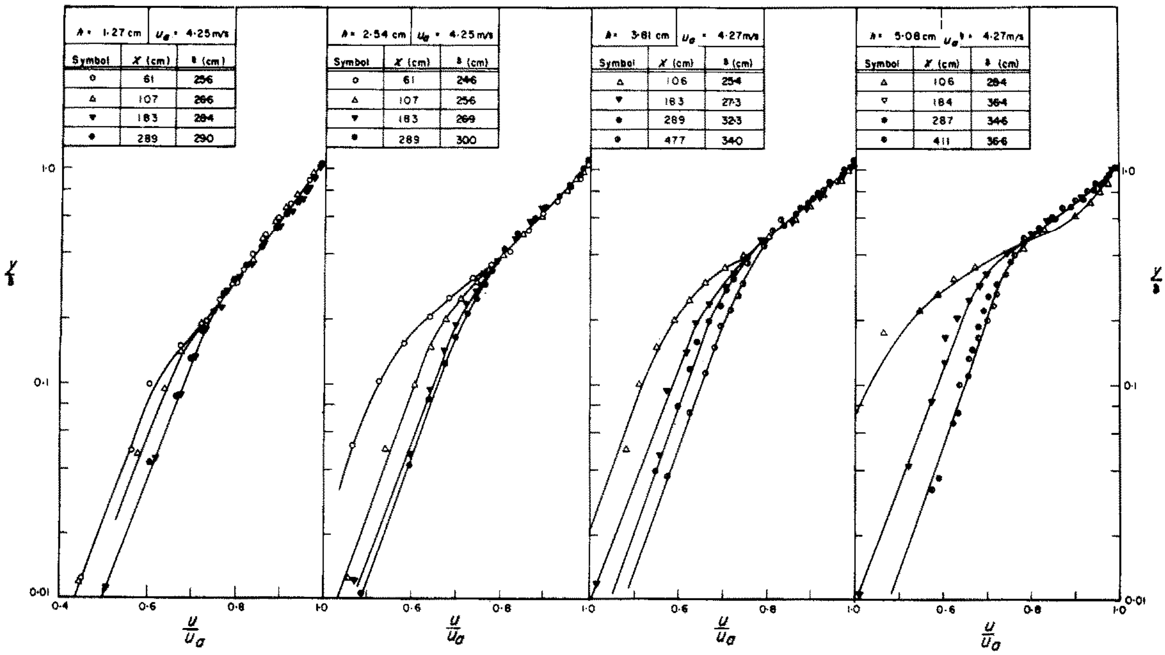

FIG. 3. Dimensionless velocity distributions.

the dimensionless distances y/δ, where δ is the height of the outer boundary layer. δ has been defined as the distance at which the local velocity has a magnitude of 0·98 u_a. Small adjustments in δ were made in order to bring the outer parts of the velocity profiles for all distances X into good agreement. As is readily seen, at large distances X, each profile consists of two well-defined logarithmic parts, separated by a blending region the height of which increases with increasing distance X.

In order to obtain an expression for the velocity distribution of the total boundary layer, one must obtain suitable equations which describe the velocity distributions in the inner and outer layer. For the outer layer, the velocity profile can be described by a type of velocity defect law

$$\frac{u - 0{\cdot}98u_a}{u_{*o}} = \frac{1}{k}\ln\frac{y}{\delta} \tag{5}$$

where u_{*o} is the shear velocity of the outer layer. The quantity u_{*o} reflects the effect of the fence on the shear stress in the outer part of the boundary layer. The outer profile develops as if a rough boundary had existed at some distance upstream from the location of the reattachment point. This "equivalent rough boundary" has a friction coefficient defined by

$$c_f = \frac{2u_{*o}^2}{u_a^2},$$

which must depend on the fence characteristics. The coefficient c_f is dependent on an empirical parameter A, defined by Plate through the relation $c_f = 0{\cdot}0544\, A^2$ [10]. Experimental data of Plate have been used to show the dependency of the coefficient A on the ratio of h/δ_o in Fig. 4, where δ_o is the thickness of the undisturbed boundary layer at the location of the fence (i.e. before the fence has been placed into the boundary layer).

For the inner profile, the assumption can be made that the shear stress at the floor is equal to that of the flow before the fence is introduced [1]. This assumption is required in order to assign

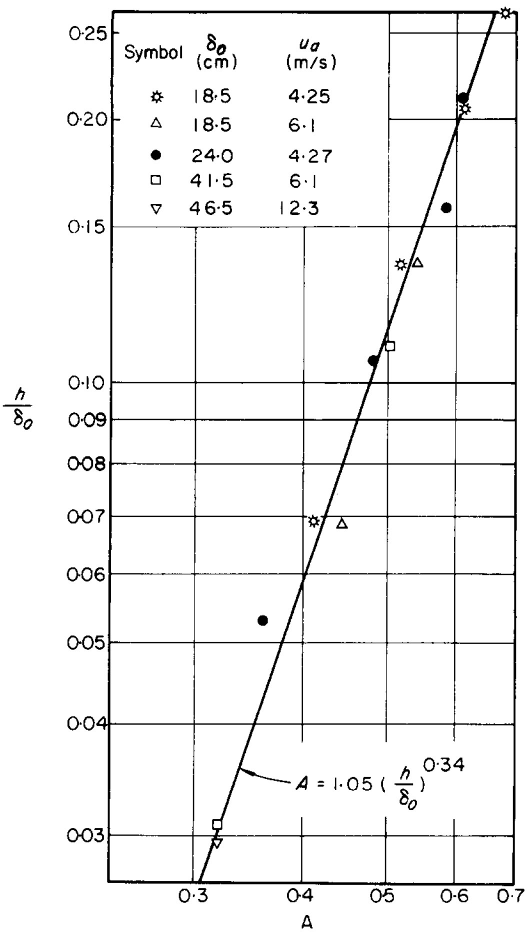

FIG. 4. A as function of h/δ_0.

a finite magnitude to the drag which is introduced by the fence. Thus, the profile can be described by the inner velocity distribution law, or the wall law, for boundary layers on smooth flat plates:

$$\frac{u}{u_{*i}} = \frac{1}{k}\ln y + D, \tag{6}$$

where the term D has to be determined from the joining condition that at the edge of the inner boundary layer, at $y = \delta'$, the inner profile velocity equals that of the outer profile. The shear velocity u_{*i} can be calculated from standard curves, for example, reference [5], p. 504. Thus, with A given by Fig. 4, and the profiles of the inner and outer boundary layer determined by equations (5) and (6), the velocity distribution of the whole boundary layer is known if the laws are given which determine the growth of the inner boundary layer, and of the outer boundary layer.

The edge δ' of the inner boundary layer can be found by extending the straight lines in Fig. 3 until inner and outer profiles intersect. From Fig. 3, it is seen that, for large values of X, u/u_a reaches a constant value of 0·75 for all fence heights. This empirical result implies that δ'/δ is constant, with the constant given from the law of the outer profile

$$\frac{u}{u_a} = \frac{u}{u_{*o}}\sqrt{\left(\frac{c_f}{2}\right)} = 0{\cdot}75 \rightarrow \frac{1}{k}\sqrt{\left(\frac{c_f}{2}\right)}\ln\frac{\delta'}{\delta}$$

$$= -\,0{\cdot}23$$

or

$$\frac{\delta'}{\delta} = \exp\left[-\frac{0{\cdot}124}{\sqrt{(c_f)}}\right]. \tag{7}$$

Equation (7) makes it possible to obtain the velocity distribution law for the disturbed boundary layer, at large distances from the fence, from a knowledge of the wall shear stress and of the boundary-layer thickness. Since at $y = \delta'$ both equations (5) and (6) are valid, D is found from the conditions:

$$\frac{u_{*i}}{k}\ln\delta' + u_{*i}D = \frac{u_{*o}}{k}\ln\frac{\delta'}{\delta} + 0{\cdot}98\,u_a$$

and with $k = 0{\cdot}38$ one finds the velocity distribution law for the total boundary layer, expressed in terms of u_a:

$$\left.\begin{aligned} y < \delta\,.\exp\left[-\frac{0{\cdot}124}{\sqrt{(c_f)}}\right]&: \frac{u}{u_a} = \frac{u_{*i}}{ku_a}\ln\frac{y}{\delta} \\ &+ 0{\cdot}75 + 0{\cdot}23\frac{u_{*i}}{u_{*o}} \\ y > \delta\,.\exp\left[-\frac{0{\cdot}124}{\sqrt{(c_f)}}\right]&: \frac{u}{u_a} = \frac{u_{*o}}{ku_a}\ln\frac{y}{\delta} + 0{\cdot}98. \end{aligned}\right\} \tag{8}$$

Since the shear velocity u_{*i} corresponds to that found at X with an undisturbed boundary layer, and since u_{*o} is determined by the ratio of h/δ_o, the velocity distribution law is fully specified at large distances X, if δ is known.

Empirically, δ is given by Fig. 5. Large increases of δ with fence height are found. The strong growth of the boundary layer is probably due to the fact that the ratio of the boundary-layer thickness δ_o ($= 13$ cm) of the undisturbed flow to fence height h is fairly small. One must expect that the boundary layer would experience a much reduced growth rate if this ratio is increased.

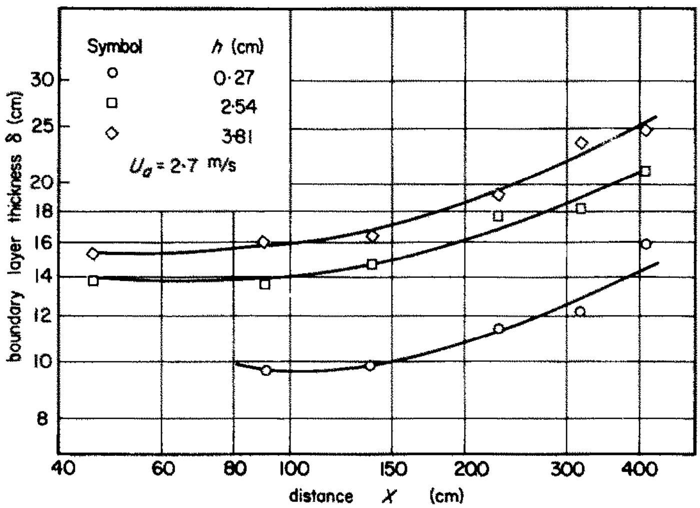

FIG. 5. Boundary-layer thickness δ as function of x.

CONCENTRATION DISTRIBUTIONS IN THE DISTURBED BOUNDARY LAYER

The measured parameters of the concentration distributions are tabulated in Table 1. Examples of concentration distributions of the ammonia gas in the disturbed boundary layer are shown in dimensionless form in Fig. 6. The length coordinate y has been made dimensionless by dividing it through λ. The concentrations have been divided by the ground level concentration c_{max}. Except for the data corresponding to short distances X, the results confirm a similarity law for the concentrations in the disturbed boundary layer. For small X, the profiles show small changes near the floor. It is found that in the separation bubble, the vertical concentrations are essentially constant, with a magnitude given by the concentrations near the separation streamline.

The similarity profiles for large distances X can be expressed well by equation (3). However, an exponent α of 1·6, fits the data better than the value of 1·8 found by Malhotra and Cermak [11]. The exponent α was first obtained by a computer using a method of least squares, but the data at large values of y/λ introduced too strong a bias on the computer calculations. Therefore, the exponent was determined from a graphical presentation of equation (3), as is shown in the example of Fig. 7.

With the concentration distributions expressed through equation (3), one must determine the scale parameters λ and c_{max} in order to fully specify the concentration distribution. In the following discussion, the growth of λ

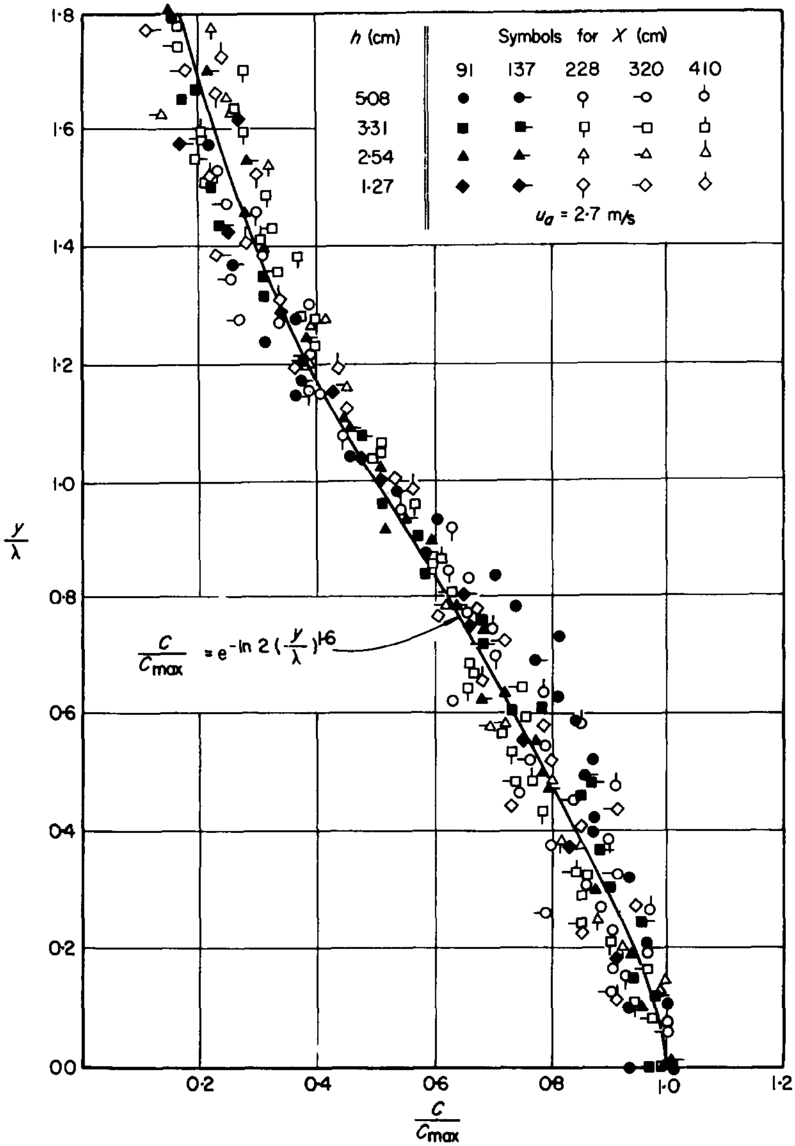

FIG. 6. Dimensionless concentration profiles.

Table 1

h_2 (cm)	X (cm)	$\lambda u_a c_{max}/G$	u_a (m/s)	λ (cm)	c_{max} (—) $\times 10^6$	c_{max}/G (s cm/cm³) $\times 10^3$
1·27	46	2·73	2·74	3·7	657	2·70
	92		2·74	5·2	532	1·92
	137		2·74	6·0	346	1·67
	228		2·74	6·3	309	1·58
	318		2·65	9·3	263	1·12
	408		2·79	10·3	229	0·95
2·54	92	2·83	2·89	6·3	350	1·56
	137		2·85	7·5	290	1·33
	228		2·74	9·8	245	1·05
	318		2·79	13·0	178	0·78
	408		2·85	12·2	153	0·82
3·81	46	2·89	2·94	8·5	518	1·15
	92		2·74	8·5	327	1·24
	137		2·74	10·6	281	1·00
	228		2·74	11·7	224	0·91
	318		2·67	15·2	179	0·73
5·08	46	2·94	2·74	12·9	458	0·84
	92		2·86	13·1	242	0·78
	137		2·67	14·0	219	0·79
	228		2·71	15·0	153	0·71
	318		2·71	20·0	123	0·54
	408		2·71	22·0	120	0·49

shall be related for the final zone to the growth of the boundary-layer thickness δ. The velocity and concentration distribution laws, δ as function of X, and the total diffused mass are then used to calculate the decrease of ground level concentration with distance.

In agreement with experimental results of other investigators, for example Poreh and Cermak [4], the length scale λ should be a function of x, where x is the distance from the source. However, when the effect of the fence on the flow is taken into consideration, it is realized that the strong shear at the sharp edge of the fence generates such a high turbulence level that all spreading that had taken place before the diffusion cloud reached the fence edge is insignificant compared to that which occurs downstream from the fence. Therefore, the diffusion cloud should behave somewhat like a diffusion cloud emitted from an elevated line source, with an elevation of the order of the fence height and located at $X = 0$. For this reason, λ was plotted against X in Fig. 8.

The fence height strongly influences the initial growth of the diffusion cloud. In the logarithmic presentation of Fig. 8, curves corresponding to increased fence heights are shifted parallel to the curve for zero fence height, with equal increments in height causing equal logarithmic increments in λ. This implies that λ increases exponentially with the fence height. A sharp-edged fence is, therefore, a very efficient device for rapidly spreading out gas clouds.

With increasing distances X, the diffusion cloud grows slower than according to a power law with an exponent of 0·8. It is not certain whether this is attributable only to the decaying turbulence level, because, for the present data, the growth of the diffusion cloud is restricted by the edge of the boundary layer. In order to illustrate this point, the ratio λ/δ was noted on each of the data points, and it is seen that the

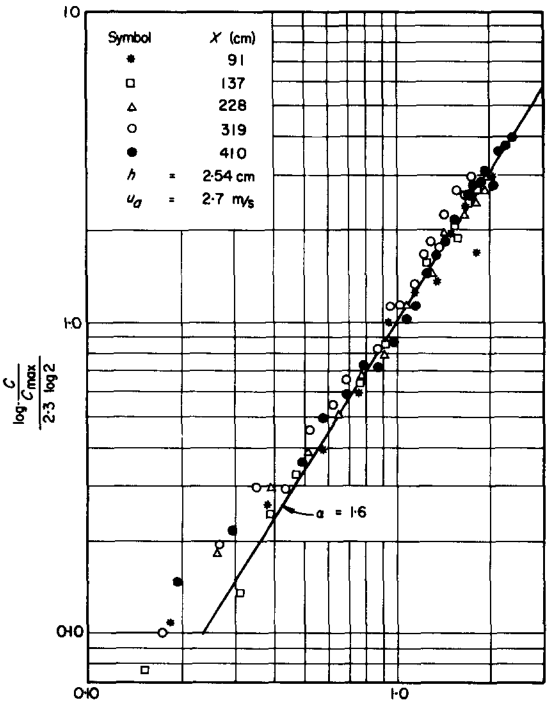

FIG. 7. Example for the determination of the exponent α.

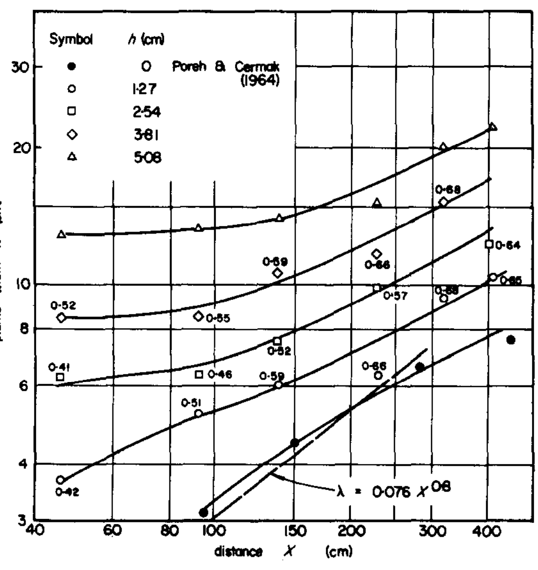

FIG. 8. The plume width λ as function of x.

data reach a constant λ/δ ratio of about 0·68 already at fairly short distances X.

With the length scale λ proportional to δ, the ground level concentrations can be calculated by considering the mass conservation equation

$$G = \int_0^\infty u \, . \, c \, \mathrm{d}y \tag{9}$$

where G is the gas discharge of the line source per unit width and unit time. The upper limit of the integral can be replaced by δ without great error. Inserting the similarity laws for velocity and concentration distributions, equations (8) and (3), into equation (9) yields:

$$G = \delta u_a c_{\max} \left[\int_0^{\delta'/\delta} \exp\left[-\ln \left(\frac{y}{\lambda}\right)^{1\cdot6} \right] \times \left\{ \frac{u_{*i}}{k u_a} \ln \frac{y}{\delta} + 0\cdot75 + 0\cdot23 \frac{u_{*i}}{u_{*o}} \right\} \mathrm{d}\left(\frac{y}{\delta}\right) + \int_{\delta'/\delta}^{1} \exp\left[-\ln 2 \left(\frac{y}{\lambda}\right)^{1\cdot6} \right] \left\{ \frac{u_{*o}}{k u_a} \ln \frac{y}{\delta} + 0\cdot98 \right\} \times \mathrm{d}\left(\frac{y}{\delta}\right) \right].$$

For the final zone, $\delta'/\delta = x'$ is given by equation (7), and $\lambda = 0\cdot68\,\delta$. In terms of these variables, equation (9) becomes:

$$G = \delta u_a c_{\max} \left\{ \frac{u_{*o}}{k u_a} \left[I_1'(x') \left(\frac{u_{*i}}{u_{*o}} - 1 \right) + I_1'(1) \right] + 0\cdot23 \left(\frac{u_{*i}}{u_{*o}} - 1 \right) I_2(x') + 0\cdot98\, I_2(1) \right\} \tag{10}$$

where

$$I_1'(x') = \int_0^{x'} \exp\left[-1\cdot29 \left(\frac{y}{\delta}\right)^{1\cdot6} \right] \ln \frac{y}{\delta} \, \mathrm{d}\left(\frac{y}{\delta}\right) = 0\cdot435\, I_1(x')$$

and

$$I_2(x') = \int_0^{x'} \exp\left[-1\cdot29 \left(\frac{y}{\delta}\right)^{1\cdot6} \right] \mathrm{d}\left(\frac{y}{\delta}\right).$$

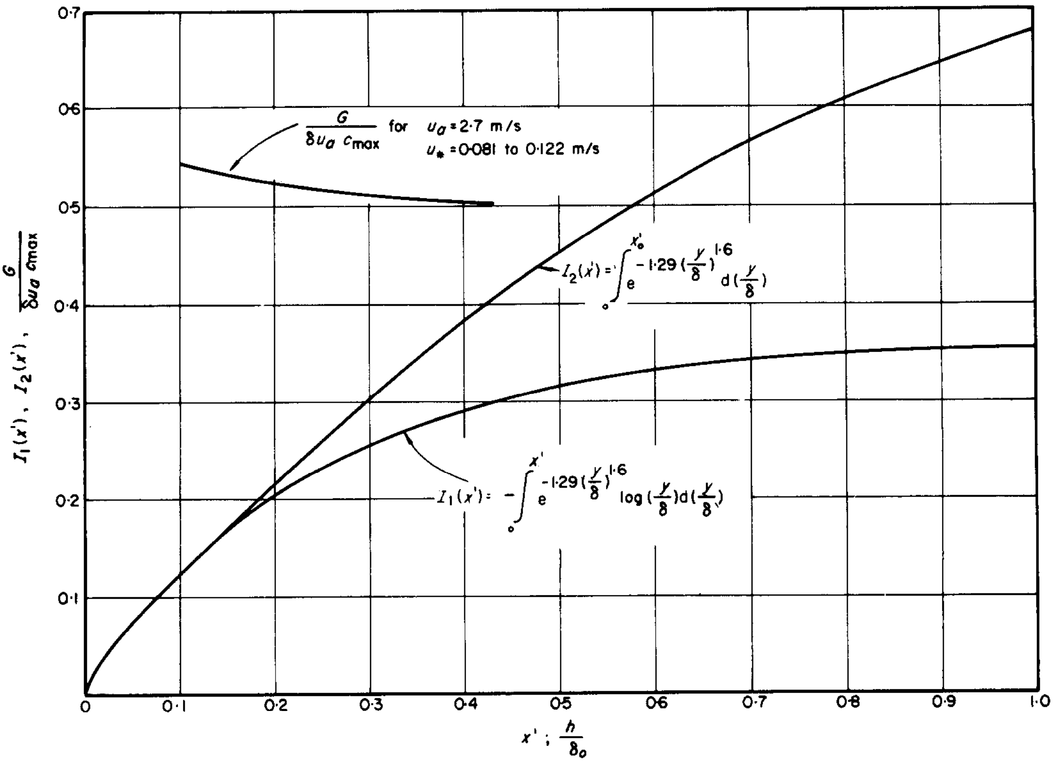

FIG. 9. Functions for calculating the ground concentrations.

The integrals I_1 and I_2 have been determined numerically and are plotted in Fig. 9.

From equation (10), the ground level concentrations were calculated. It was found that for the experimental data the effect of u_{*i} was very small. Since u_{*i} was not known, values of $G/\delta\, u_a\, c_{max}$ were calculated with u_{*i} ranging from 8·5 to 11·6 cm/s. The variation in $G/\delta\, u_a\, c_{max}$ was found to be less than 1 per cent over this range of u_{*i}-values, while it changed from 0·50 to 0·54 with increase in the fence heights considered. The ground level concentration was calculated from the results by using experimental values of u_a and λ as given in Table 1. The results are compared with the experimentally found c_{max} values in Fig. 10. Except for the highest concentrations, which are found at short distances X, the agreement of the experimental data with the calculated data is good. All the data fall within the band given by the likely error of

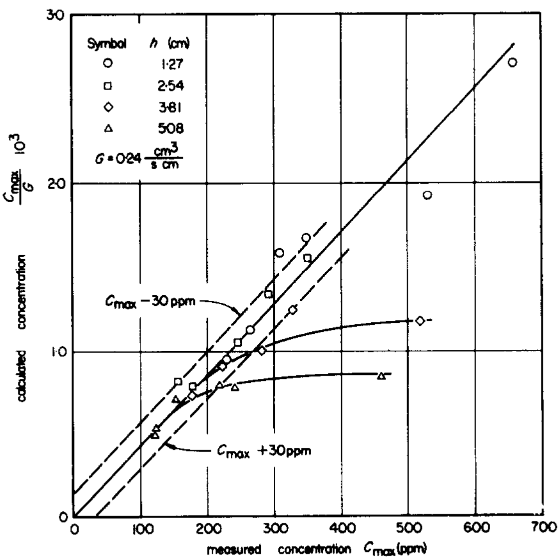

FIG. 10. Comparison of calculated and measured maximum concentration.

± 30 ppm. It is thus demonstrated that the ground level concentration in the final zone can be calculated from the simple concentration distribution law equation (3), the development of the boundary-layer thickness, and the velocity distribution law equation (8).

ACKNOWLEDGEMENTS

Financial support for this study has been given by the Agricultural Research Service under Contract No. 12-14-100-45 46 (41) and by the U.S. Army, Fort Huachuca, under Grant No. DA-SIG-36-039-62-G24. H. Shokouh, A. A. Quraishi and R. D. Marshall helped with gathering the experimental data. Valuable comments by Dr. J. Deardorff are gratefully acknowledged.

REFERENCES

1. G. I. Taylor, Diffusion by continuous movement, *Proc. Lond. Math. Soc.* **20**, 196–212 (1921).
2. F. H. Clauser, The turbulent boundary layer, in *Advances in Applied Mechanics*, Vol. 4. Academic Press, New York (1956).
3. K. Wieghardt, Über Ausbreitungsvorgänge in turbulenten Reibungsschichten, *Z. Angew. Math. Mech.* **28**, 346–355 (1948).
4. M. Poreh and J. E. Cermak, Study of diffusion from a line source in a turbulent boundary layer, *Int. J. Heat Mass Transfer* **7**, 1083–1095 (1964).
5. H. Schlichting, *Boundary-layer Theory*, 4th edn., McGraw-Hill, New York (1960).
6. W. P. Elliott, The growth of the atmospheric internal boundary layer, *Trans. Am. Geophys. Un.* **39**, 1048–1054 (1958).
7. J. E. Cermak, Lagrangian similarity hypothesis applied to diffusion in turbulent shear flow, *J. Fluid Mech.* **15** (1), 49–64 (1963).
8. A. A. Townsend, Self-preserving flow inside a turbulent boundary layer, *J. Fluid Mech.* **22**, 773–797 (1965).
9. A. A. Townsend, The response of a turbulent boundary layer to abrupt changes in surface conditions, *J. Fluid Mech.* **22**, 799–822 (1965).
10. E. J. Plate, Ein Beitrag zur Berechnung von Austauschvorgängen in der durch eine Wand gestorten bodennahen Luftschicht. Doctoral dissertation, Department of Civil Engineering, Technische Hochschule Stuttgart, Stuttgart, Germany (1966).
11. R. C. Malhotra and J. E. Cermak, Mass diffusion in neutral and unstably stratified boundary-layer flows, *Int. J. Heat Mass Transfer* **7**, 169–186 (1964).
12. H. S. Nagabhushanaiah, Separation flow downstream of a plate set normal to a plane boundary, Ph.D. Dissertion, Civil Engr. Dept, Colorado State University, Fort Collins, Colorado (1964).

Résumé—On discute le champ de concentration existant loin à l'amont d'une source linéaire de gaz ammoniac qui émet continuellement dans la couche limite sur une plaque plane lisse. La couche limite est arrêtée par une barrière imperméable à bord vif qui s'étend sur toute la largeur de la plaque à une courte distance de la source. La base de la discussion est un ensemble de données expérimentales obtenues dans une soufflerie.

L'écoulement à l'aval de la barrière présente trois zones différentes de distributions de vitesse. Ces zones sont indiquées et l'on donne une loi de distribution de vitesse basée sur l'hypothèse que la couche limite perturbée est constituée de deux parties: une couche extérieure pour laquelle les paramètres de la loi de distribution dépendent de l'épaisseur de la couche limite et de la géométrie de la barrière qui la perturbe, et une couche intérieure pour laquelle la loi de distribution de vitesse dépend de la rugosité de la paroi.

Les distributions verticales de concentrations à l'aval de la barrière suivent une loi de similitude dont la forme correspond à celle trouvée avec les couches limites non perturbées. Les paramètres de similitude reflètent fortement la présence de la barrière. La longueur caractéristique λ augmente exponentiellement avec la hauteur de la barrière. La longueur caractéristique, la loi de similitude et la distribution de vitesse sont utilisées pour calculer les concentrations maximales au sol à de grandes distances en aval de la barrière où la présence de la frontière de la couche limite empêche le panache de diffusion de croître au-delà de cette couche limite.

Zusammenfassung—Eine linienförmige Quelle emittiert kontinuierlich Ammoniakgas in die Grenzschicht entlang einer glatten ebenen Platte. Das Konzentrationsfeld, das in grösserer Entfernung stromabwärts von der Quelle existiert, wird diskutiert. Die Grenzschicht wird durch ein undurchlässiges, scharfkantiges Hindernis, das sich über die gesamte Breite der Platte erstreckt und sich in geringer Entfernung stromabwärts von der Quelle befindet, gestört. Als Grundlage der Betrachtung dient eine Reihe von Versuchsdaten, die in einem Windkanal gewonnen wurden.

Das Strömungsfeld stromabwärts vom Hindernis weist drei verschiedene Zonen der Geschwindigkeitsverteilung auf. Diese Zonen werden aufgezeigt und ein Gesetz für die Geschwindigkeitsverteilung wird angegeben. Dieses Gesetz gründet sich auf die Annahme, dass die gestörte Grenzschicht aus zwei Schichten besteht: Aus einer äusseren Schicht, für deren Geschwindigkeitsverteilung die Dicke der Grenzschicht und die Geometrie des Hindernisses massgebend sind, und aus einer inneren Schicht, deren Geschwindigkeitsverteilung von der Rauhigkeit der Plattenoberfläche abhängt.

Der Konzentrationsverlauf senkrecht zur Platte folgt für alle stromabwärts vom Hindernis gelegenen Stellen einem Ähnlichkeitsgesetz entsprechend dem, das in ungestörten Grenzschichten gefunden wurde. Aus den Ähnlichkeitskenngrössen folgt deutlich das Vorhandensein des Hindernisses. Es ergab sich, dass die charakteristische Länge λ exponentiell mit der Höhe des Hindernisses anwächst. Die charakteristische Länge, das Ähnlichkeitsgesetz und das Gesetz für die Geschwindigkeitsverteilung werden dazu verwendet, die maximalen Konzentrationen an der Plattenoberfläche stromabwärts in grosser Entfernung vom Hindernis zu berechnen, wo das Ende der Grenzschicht das Anwachsen des Diffusionsfeldes auf das der Grenzschicht beschränkt.

Аннотация—Рассматривается поле концентрации далеко вниз по потоку от линейного источника аммиака, поступающего непрерывно в пограничный слой вдоль гладкой плоской пластины. Пограничный слой прерывается по всей ширине пластины непроницаемой перегородкой с острой кромкой, помещенной на небольшом расстоянии от источника. Анализируются экспериментальные данные, полученные в аэродинами ческой трубе.

Вниз по потоку от перегородки обнаружены три области распределения скоростей. Законы распределения в них основаны на предположении, что возмущенный пограничный слой состоит из двух частей: наружного слоя, в котором закон распределения скоростей зависит от толщины пограничного слоя и конфигурации перегородки, и внутреннего слоя, для которого закон распределения скорости зависит от шероховатости основания.

Поперечный профиль концентрации вниз по потоку от перегородки подчиняется аналогичному по записи закону для невозмущенных пограничных слоев. В параметры подобия входят размеры перегородки. Найдено, что характеристическая длина увеличивается экспоненциально с возрастанием высоты перегородки. Характеристичекая длина, закон подобия, закон распределения скоростей используются для расчета максимальных концентраций на поверхности далеко вниз по потоку от перегородки, где наличие кромки пограничного слоя препятствует распространению диффузии за пределы пограничного слоя.